



**HAL**  
open science

# Assessing the impact of non-compliant users response to System-Optimal Dynamic Traffic Assignment

Enrico Siri, Paola Goatin

► **To cite this version:**

Enrico Siri, Paola Goatin. Assessing the impact of non-compliant users response to System-Optimal Dynamic Traffic Assignment. CDC 2023 - 62nd IEEE Conference on Decision and Control, Dec 2023, Singapore, Singapore. pp.7785-7790, 10.1109/CDC49753.2023.10383488 . hal-04206328

**HAL Id: hal-04206328**

**<https://hal.science/hal-04206328v1>**

Submitted on 13 Sep 2023

**HAL** is a multi-disciplinary open access archive for the deposit and dissemination of scientific research documents, whether they are published or not. The documents may come from teaching and research institutions in France or abroad, or from public or private research centers.

L'archive ouverte pluridisciplinaire **HAL**, est destinée au dépôt et à la diffusion de documents scientifiques de niveau recherche, publiés ou non, émanant des établissements d'enseignement et de recherche français ou étrangers, des laboratoires publics ou privés.

# Assessing the impact of non-compliant users response to System-Optimal Dynamic Traffic Assignment

Enrico Siri and Paola Goatin

**Abstract**—In the present work, we address a pseudo - System Optimum Dynamic Traffic Assignment optimization problem on road networks relying on trajectory control over a portion of the flows and limited knowledge on user response. The fractions of controlled flow moving between each origin-destination couple are defined as “compliant”, while the remaining portions, consisting of users free to make their own individual choices, are defined as “non-compliant”. The objective is to globally improve the state of the network by controlling a varying subset of compliant traffic flows. A Godunov discretization of the Lighthill-Williams-Richards model coupled with a triangular fundamental diagram is employed as the flow dynamics model. At junctions, a multi-class solver is applied which requires a class-density-weighted aggregate distribution matrix and incoming links priorities. On one hand, the selfish response of non-compliant users to changing traffic conditions is computed at each time step by updating the class related turn ratios accordingly to a discrete-choice multinomial Logit model to represent users imperfect information. On the other hand, the control action is actuated by varying the flow rates over a pre-computed set of routes while the coupled optimization problem takes into account an a priori fixed distribution of users at the nodes. We show how the effectiveness of the resulting finite horizon optimal control problem degrades by not considering the dynamic response of non-compliant users and how it varies according to the fraction of compliant ones.

## I. INTRODUCTION

The problem of *Dynamic Traffic Assignment* (DTA), consisting in optimally allocating origin-destination routes depending of traffic demand in order to alleviate congestion on a given road network, has been widely studied over the last decades [1], [2]. In particular, we can distinguish between *user equilibrium* (UE) strategies [3], in which users seek to minimize their individual travel times, often leading to inefficient network utilization [4], and *system optimal* (SO) allocations, where users are routed based on the output of a global optimization algorithm which minimizes the total travel time, leading to efficient network use [5], [6]. Of course, SO-DTA efficacy is hard to obtain in practice, since users tend to target the selfish individual travel time minimization and may not be willing to comply with external rules in the common interest. Yet, partial SO-DTA can be implemented by controlling a fraction of drivers (for example through some incentives) referred to as *compliant*, either assuming that *non-compliant* users keep their original routing scheme [6] or react to the changes adapting their strategy, thus leading to a Stackelberg games [7], [8] if the controller is able to anticipate the reaction. These problems are usually

considered in a static framework under strongly simplifying assumptions. Yet, practical implementation often requires a dynamic setting, for example in the case of temporary network disruptions [9], [6]. Moreover, the recent deployment of navigation devices (e.g. Google Maps or Waze) gives non-compliant users the possibility to react to traffic conditions almost in real time.

This paper aims to provide the tools to address the SO-DTA with partial control and reacting non-compliant users in a macroscopic and non-stationary framework. Macroscopic multi-population traffic flow models have been developed in recent years to describe the interactions among different classes of vehicles such as cars and trucks [10], cars and motorcycles [11], [12] or even among human driven and autonomous vehicles [13]. The approach has also been extended to road networks [14]. In particular, in [15] each population is identified by its origin and destination, while [16] and [6] describe populations moving on predefined paths. In this work, following [17], [4], we include the case of drivers adapting their route dynamically to minimize their travel times based on information about the current state of the network.

We propose a multi-population traffic flow model on networks, in which the flow of each population is governed by the corresponding mass conservation equation on road segments (summing up into the standard Lighthill-Williams-Richards (LWR) model [18]). The different populations are characterized by their split ratios at junctions, that can be either pre-defined and fixed (e.g. for the compliant users) or adjust to the traffic conditions to minimize travel times to destination (for non-compliant drivers). In this way, different routing strategies can be taken into account, resulting in possibly time-dependent split ratios at road junctions. We note that, at the moment, we do not consider any forecast ability for the future states of the system.

The implementation of our model allows investigating the effectiveness of a system-optimal routing control strategy at different penetration rates of the compliant class and under different assumptions regarding non-compliant users’ behaviour. The rest of the paper is organized as follows. In Section II, we present the multi-population traffic flow model. In Section III, we describe the assumptions about user classes and the routing strategies they apply, while in Section IV the associated optimization problem and some numerical results are reported.

E. Siri and P. Goatin are with Université Côte d’Azur, Inria, CNRS, LJAD, 2004, route des Lucioles - BP 93 06902 Sophia Antipolis Cedex, FRANCE; {enrico.siri, paola.goatin}@inria.fr

## II. A GENERAL MULTI-POPULATION TRAFFIC FLOW MODEL ON NETWORKS

We consider a road network modeled by an oriented graph consisting of a finite set of arcs  $\mathcal{I} := \{I_\ell\}_{\ell \in \mathcal{L}}$ , parameterized by segments  $I_\ell = \pi_\ell ]0, L_\ell[$ , connected at nodes  $J_k \in \mathcal{J}$ ,  $k = 1, \dots, K$ . Given  $J_k \in \mathcal{J}$ , we denote by  $Inc(J_k) := \{i \in \mathcal{L} : J_k \in I_i, \pi_i(L_i) = J_k\}$  the set of incoming roads at  $J_k$ , and by  $Out(J_k) := \{j \in \mathcal{L} : J_k \in I_j, \pi_j(0) = J_k\}$  the set of outgoing roads. Moreover we denote by  $\mathcal{O}$ ,  $\mathcal{D} \subset \mathcal{J}$  respectively the *origin* and *destination nodes*.

The macroscopic framework used to describe the flow of different classes of users on a road network is based of a set of coupled conservation equations on each link, together with suitable transmission conditions at junctions. In particular, each class density  $\rho^c$ ,  $c = 1, \dots, N_c$ , is characterized by specific, possibly time-dependent, distribution coefficients at junctions, which will be computed according to the class specific routing strategy in Section III.

### A. Traffic dynamics on arcs

The traffic dynamics on each road is described by a LWR-type model in its discrete CTM version [19], [4], [6], corresponding to flow functions of the form  $\rho^c v_\ell(r)$ , where  $r = \sum_{c=1}^{N_c} \rho^c \in [0, R_\ell]$  is the total traffic density, and the speed function  $v_\ell : [0, R_\ell] \rightarrow [0, V_\ell]$  is a non-increasing function such that  $v_\ell(0) = V_\ell$  and  $v_\ell(R_\ell) = 0$ . Moreover, we assume that there exists a unique point  $\hat{r}_\ell \in ]0, R_\ell[$  such that the flow function  $\rho \mapsto \rho v_\ell(\rho)$  is increasing for  $\rho \in [0, \hat{r}_\ell[$  and decreasing for  $\rho \in ]\hat{r}_\ell, R_\ell]$ .

We divide each arc  $I_\ell$  uniformly in  $N_\ell$  cells of size  $\Delta x_\ell = L_\ell/N_\ell$ . Given an initial density distribution  $\bar{\rho}_{\ell,h}^c$ ,  $h = 1, \dots, N_\ell$ ,  $c = 1, \dots, N_c$ , at each time step  $t^\nu = \nu \Delta t$ ,  $\nu \in \mathbb{N}$ , we update the class-specific traffic density using the conservative scheme

$$\rho_{\ell,h}^{c,\nu+1} = \rho_{\ell,h}^{c,\nu} - \frac{\Delta t}{\Delta x_\ell} \left( \frac{\rho_{\ell,h}^{c,\nu}}{r_{\ell,h}^\nu} F_{\ell,h}^\nu - \frac{\rho_{\ell,h-1}^{c,\nu}}{r_{\ell,h-1}^\nu} F_{\ell,h-1}^\nu \right), \quad (1)$$

for  $h = 2, \dots, N_\ell - 1$ , where  $F_{\ell,h}^\nu$  is the standard *Godunov flow* [20] corresponding to  $f_\ell(r) = r v_\ell(r)$ , defined by

$$F_{\ell,h}^\nu = F_\ell(r_{\ell,h}^\nu, r_{\ell,h+1}^\nu) := \min \{ D_\ell(r_{\ell,h}^\nu), S_\ell(r_{\ell,h+1}^\nu) \}. \quad (2)$$

Above,  $D_\ell(\rho) = f_\ell(\min\{r, \hat{r}_\ell\})$  and  $S_\ell(\rho) = f_\ell(\max\{r, \hat{r}_\ell\})$  are the (total) demand and supply functions, respectively [21].

Similarly, the densities in the first and last cells are computed according to the incoming and outgoing fluxes, respectively  $\bar{\gamma}_{\ell,1}^{c,\nu}$  and  $\bar{\gamma}_{\ell,N_\ell}^{c,\nu}$ , which depend on the upstream and downstream node dynamics, see Section II-B. We set:

$$\rho_{\ell,1}^{c,\nu+1} = \rho_{\ell,1}^{c,\nu} - \frac{\Delta t}{\Delta x_\ell} \left( \frac{\rho_{\ell,1}^{c,\nu}}{r_{\ell,1}^\nu} F_{\ell,1}^\nu - \bar{\gamma}_{\ell,1}^{c,\nu} \right), \quad (3)$$

$$\rho_{\ell,N_\ell}^{c,\nu+1} = \rho_{\ell,N_\ell}^{c,\nu} - \frac{\Delta t}{\Delta x_\ell} \left( \bar{\gamma}_{\ell,N_\ell}^{c,\nu} - \frac{\rho_{\ell,N_\ell-1}^{c,\nu}}{r_{\ell,N_\ell-1}^\nu} F_{\ell,N_\ell-1}^\nu \right). \quad (4)$$

To guarantee the stability of the scheme (1)-(4), we impose the usual Courant-Fredrichs-Lewy (CFL) condition [22]

$$\Delta t \leq \frac{\Delta x_\ell}{\max_\ell \|f'_\ell\|_{L^\infty}([0, R_\ell])}. \quad (5)$$

### B. Coupling conditions at junctions

Let the (possibly time dependent) distribution matrices at any junction  $J_k$  be given for each class  $\rho^c$ ,  $c = 1, \dots, N_c$

$$A_k^{c,\nu} = \left\{ a_{k,ji}^{c,\nu} \right\}_{i,j}, \quad i \in Inc(J_k), j \in Out(J_k),$$

such that

$$a_{k,ji}^{c,\nu} \geq 0 \quad \text{for any } i, j \quad (6)$$

and

$$\sum_{j \in Out(J_k)} a_{k,ji}^{c,\nu} = 1 \quad \text{for all } i \in Inc(J_k), \quad (7)$$

which ensure the flow conservation at junctions.

We construct the total traffic distribution matrix as

$$A_k^\nu := \{a_{k,ji}^\nu\}, \quad \text{where} \quad a_{k,ji}^\nu := \sum_{c=1}^{N_c} a_{k,ji}^{c,\nu} \frac{\rho_{i,N_i}^{c,\nu}}{r_{i,N_i}^\nu} \quad (8)$$

defines the weighted distribution coefficients depending on the density ratios in the last cells of the incoming roads.

Using any prescribed junction rules applied to the matrices  $A_k^\nu$  (see e.g. [23] for an overview on *Riemann Solvers at junctions*), one can compute the total fluxes exiting the incoming roads

$$\bar{\gamma}_{i,N_i}^\nu, \quad i \in Inc(J_k),$$

which are then redistributed among the various classes  $c = 1, \dots, N_c$ : g

$$\bar{\gamma}_{i,N_i}^{c,\nu} = \frac{\rho_{i,N_i}^{c,\nu}}{r_{i,N_i}^\nu} \bar{\gamma}_{i,N_i}^\nu, \quad i \in Inc(J_k), \quad (9)$$

$$\bar{\gamma}_{j,1}^{c,\nu} = \sum_{i \in Inc(J_k)} a_{k,ji}^{c,\nu} \bar{\gamma}_{i,N_i}^{c,\nu}, \quad j \in Out(J_k), \quad (10)$$

providing the boundary flows to be used in (4) and (3), respectively.

In this work, we will apply the *Priority Riemann Solver* introduced in [24], which can handle an arbitrary number of incoming and outgoing roads, accounting for priorities among the incoming roads and maximizing the through flow.

### C. Inflow and outflow boundary conditions

We denote by  $\text{Fin}_o^\nu = \sum_{c=1}^{N_c} \text{fin}_o^{c,\nu}$  the total amount of incoming flows about to enter the network from an origin node  $J_o$  at time  $t = t^\nu$  which depends on the class-specific incoming flows  $\text{fin}_o^{c,\nu}$ .

Since the inflow to the network is limited by the residual capacity of the first cells on each arc  $\ell \in Out(J_o)$ , the full demand  $\text{Fin}_o^\nu$  might not be accommodated. To keep track of the potential loss of demand in case of a saturated network, the most straightforward solution is relying on a *buffer* associated with each source node, defined as a cell of infinite capacity. This solves the flow conservation issue at the boundary but it may result in the repeated violation

of the FIFO condition commonly required in modelling flow propagation because we assume that the vehicles, once in a cell, are uniformly distributed no matter the arrival order. To alleviate this, one can cap the maximum capacity of a single buffer and adjust dynamically their number if necessary. A buffers sequence is then treated like a regular incoming link and each origin node like any other network junction. Thus, the total flow coming from the upstream first buffer passing through an origin node, defined by

$$\bar{\gamma}_o^\nu, \quad J_o \in \mathcal{O} \quad (11)$$

can be managed by a solver and redistributed among each class  $c$

$$\bar{\gamma}_o^{c,\nu} = \frac{l_{o,1}^{c,\nu}}{l_{o,1}^\nu} \bar{\gamma}_o^\nu \quad \bar{\gamma}_{j,1}^{c,\nu} = a_{o,j1}^{c,\nu} \bar{\gamma}_o^{c,\nu}.$$

where  $l_{o,1}^{c,\nu}$  and  $l_{o,1}^\nu$  are the total and class-specific number of vehicles in the first buffer, respectively. This provides the boundary conditions at each origin node  $J_o$ , for each class  $c$ . See [6] for a in-depth explanation of the algorithm applied to manage the no-lag inter-buffer flow propagation.

Regarding the outflow boundary conditions, it is sufficient to associate to each destination node  $J_d \in \mathcal{D}$  a *sink*, intended as a cell able to accommodate an infinite amount of vehicles over time. However, we may want to set a limit on the amount of vehicles it can accept per unit of time. Thus, we denote by  $F_{out_d}^\nu$  the total outflow boundary conditions for destination node  $J_d$  at time  $t = t^\nu$ , i.e. the maximum allowed outflow.

A destination node can thus be modelled as a junction between the incoming arcs  $\ell \in Inc(J_d)$  and a downstream sink. It is then possible to apply a solver in order to compute the total flow leaving each incoming arc

$$\bar{\gamma}_{i,N_i}^\nu, \quad i \in Inc(J_d),$$

and then redistribute it among each class  $c$

$$\bar{\gamma}_{i,N_i}^{c,\nu} = \frac{\rho_{i,N_i}^{c,\nu}}{r_{i,N_i}^\nu} \bar{\gamma}_{i,N_i}^\nu, \quad \bar{\gamma}_d^{c,\nu} = \sum_{i \in Inc(J_d)} \alpha_{d,1i}^{c,\nu} \bar{\gamma}_{i,N_i}^{c,\nu}$$

where, as a reminder,  $\rho_{i,N_i}^{c,\nu}$  and  $r_{i,N_i}^\nu$  are the class-specific and the total vehicle densities on the last cell  $N_i$  of the incoming link  $i \in Inc(J_d)$ .

### III. CLASS ROUTING STRATEGIES

We can define each class  $c = 1, \dots, N_c$  as a tuple  $(J_{o^c}, J_{d^c}, \mathcal{A}^c)$  where  $J_{o^c} \subseteq \mathcal{O}$ ,  $J_{d^c} \subseteq \mathcal{D}$  and  $\mathcal{A}^c = \{A_k^{c,\nu}\}$ . Each set  $\mathcal{A}^c$ , consisting of all distribution matrices at each node  $J_k$  and for each discrete time instant  $t^\nu$ , implicitly represents the routing strategy adopted by class  $c$  throughout the entire time horizon which, coupled with an origin-destination pair, characterize the class itself.

Let us define a strategy  $\mathcal{A}^c$  as an *admissible strategy* for the class  $c$  if at each time  $t^\nu$  and in any node  $J_k$  it ensures flow conservation and prevents the flow of the class  $c$  to be routed on any arc  $I_l \in Out(J_k)$  from which it is no longer possible to reach destination  $J_{d^c}$ . For any class  $c$  and

at each node  $J_k$ , let  $p_{k_s}^c = [J_k, \dots, J_{d^c}]$  be a path linking nodes  $J_k$  to  $J_{d^c}$  defined as an ordered sequence of nodes without repetition, in a way that for any consecutive  $J_v, J_u \in p_{k_s}^c$ ,  $\exists \ell \in \mathcal{L}$  such that  $\pi_\ell(0) = J_v$  and  $\pi_\ell(L_\ell) = J_u$ .  $\mathcal{P}_k^c = \{p_{k_s}^c\}$ . Therefore, let  $\mathcal{P}_k^c = \{p_{k_s}^c\}$  be the set of all paths that from node  $J_k$  lead to  $J_{d^c}$ , with  $s = 1, \dots, P_k^c$  and where  $P_k^c$  is the number of available paths for the class  $c$ .

For a strategy  $\mathcal{A}^c$  to be admissible, at every node  $J_k$  where  $\mathcal{P}_k^c \neq \emptyset$ , besides (6) and (7), we require that

$$a_{k,j_i}^{c,\nu} \leq \sum_{s=1}^{P_k^c} \delta_{k,j_s}^c \quad (12)$$

where

$$\delta_{k,j_s}^c = \begin{cases} 1 & \text{if } \pi_j(L_j) \in p_{k_s}^c \\ 0 & \text{otherwise.} \end{cases} \quad (13)$$

Conditions (12) coupled with (13) binds the routing of a class's flow only over arcs belonging to paths leading to the respective destination, assuming for each origin-destination pair that at least one such path exists. It should then be noted how (6)-(7) and (12)-(13) also apply to an origin node. It follows that, if an admissible strategy is applied, the flow of a class generated at an origin can only move along paths connecting its origin to its destination.

The only remaining issue in the flow routing at junctions may come from the initial conditions, if initial densities of a class  $c$  are positive on arcs from which  $J_{d^c}$  cannot be reached. To overcome this problem and without any loss of generality, let us define as *admissible initial conditions* any density pattern on arcs at  $t^0 = 0$  such that:

$$\rho_{\ell,h}^{c,0} = \begin{cases} 0 & \text{if } \mathcal{P}_k^c = \emptyset, J_k = \pi_\ell(L_\ell), \\ \bar{\rho}_{\ell,h}^c \geq 0 & \text{otherwise.} \end{cases} \quad (14)$$

As long as an admissible strategy with admissible initial conditions is applied, specifying a routing strategy for a class  $c$  at a node  $J_k$  with  $P_k^c = \emptyset$  is superfluous. This is because, whatever values the matrices  $A_k^{c,\nu}$  may assume, they have no effect on  $A_k^\nu$  defined in (8).

We now distinguish between two class sets: *compliant* and *non-compliant* users. The former describes users traveling along a unique pre-defined path while the latter representing users adopting a selfish, time varying, routing strategy.

#### A. Compliant users

A compliant class is characterized by a set  $\mathcal{A}^c$  of time-invariant distribution matrices prefiguring a routing along a unique path connecting  $J_{o^c}$  to  $J_{d^c}$ . Let us name such path  $\bar{p}^c \in \mathcal{P}_{o^c}^c$ . Therefore, the coefficients of the distribution matrices for a compliant class must satisfy (6)-(7) and the following condition for each  $J_k \in \bar{p}^c$ :

$$a_{k,j_i}^{c,\nu} = \begin{cases} 1 & \text{if } \pi_j(L_j) \in \bar{p}^c, \\ 0 & \text{otherwise.} \end{cases} \quad (15)$$

For every compliant class  $c$  we then assume that:

$$\rho_{\ell,h}^{c,0} = 0, \quad h = 1, \dots, N_\ell, \ell \in \mathcal{L}. \quad (16)$$

The distribution coefficients defined in (15) represent an admissible strategy that coupled with (16) binds compliant users to move exclusively along  $\bar{p}^c$ .

### B. Non-compliant users

A non-compliant class is characterized by a set  $\mathcal{A}^c$  of distribution matrices that depend on some function of the network state. Within the scope of the present work, users of a non-compliant class adopt a stochastic wardropian equilibrium behaviour, in order to minimize their perceived travel time based on a multinomial Logit distribution [25] at each junction. We defined as  $z_{k,s}^{c,\nu}$  the probability associated with choosing path  $p_{k,s}^c$  at junction  $J_k$  for the users of class  $c$  at time step  $\nu$ , which is computed according to

$$z_{k,s}^{c,\nu} = \frac{1}{1 + \sum_{y \neq s} e^{-\theta^c(d_{k,s}^{\nu} - d_{k,y}^{\nu})}}, \quad (17)$$

where  $d_{k,s}^{\nu}$  is the actual travel time between node  $J_k$  and node  $J_d^c$  while  $\theta^c$  can be seen as the class-specific user sensitivity coefficient to marginal variation of travel time due to choosing one route over another. It is then possible to obtain the distribution coefficients for the non-compliant class  $c$  associated with all nodes  $J_k$  whereby  $\mathcal{P}_k^c \neq \emptyset$  as follows:

$$\alpha_{k,ji}^{c,\nu} = \sum_{s=1}^{P_k^c} z_{k,s}^{c,\nu} \cdot \delta_{k,js} \quad (18)$$

where  $\delta_{k,js}$  is the link-path incidence coefficient defined in (13). Clearly (18) represents an admissible strategy. We then apply a smoothing function that adjusts the updating of the distribution matrices as follows

$$A_k^{c,\nu} = \omega^c \hat{A}_k^{c,\nu} + (1 - \omega^c) A_k^{c,\nu-1} \quad (19)$$

where  $\hat{A}_k^{c,\nu}$  is the distribution matrix for the class  $c$  obtained applying (18) and  $\omega^c \in [0, 1]$ . It follows that if  $\hat{A}_k^{c,\nu}$  and  $A_k^{c,\nu-1}$  are admissible, then necessarily  $A_k^{c,\nu}$  is admissible.

## IV. NUMERICAL RESULTS

The traffic flow model presented in this paper is implemented in Python 3.11 making use of the following main libraries: networkx [26], numpy [27] and pandas [28] while for the optimization problem, the scipy library's implementation of the differential evolution algorithm is used [29].

### A. Optimization Problem

The control action aimed at improving the overall network performance is actuated by converting at the origin nodes a fraction  $\lambda \in [0, 1]$  of non-compliant inflows into compliant ones and then routing them on the associated paths. The control vector is computed as a result of a finite horizon optimization problem. We assume  $\lambda$  as fixed during each simulation and known a priori. The paths available to each non-compliant class are computed during the initialization phase and the associated path-related compliant classes are then initialized accordingly.

In this work, we consider as performance function the total travel time of all vehicles passing through the network, i.e.

$$H^1(\bar{u}) = \sum_{\nu=1}^{N_\nu} \sum_{\ell \in \mathcal{L}} \sum_{h=1}^{N_\ell} r_{\ell,h}^\nu(\bar{u}) \Delta x_\ell \Delta t \quad (20)$$

and the total travel time of all vehicles waiting in the buffers, i.e.

$$H^2(\bar{u}) = \sum_{\nu=1}^{N_\nu} \sum_{J_o \in \mathcal{O}} \sum_{b=1}^{B_o} l_{o,b}^\nu(\bar{u}) \Delta t. \quad (21)$$

Let  $N_\nu$  be the number of simulated instants,  $\bar{u} = \{u_{o,s}^{c,\mu}\}$  the control vector and  $u_{o,s}^{c,\mu}$  the fraction of class  $c$  non-compliant users having  $J_o$  as origin node which are converted to the relative compliant one associated to path  $p_{o,s}^c \in \mathcal{P}_o^c$  at time instant  $t = t^\mu$ . The index  $\mu$  is associated with time steps  $t^\mu = \mu \Delta t'$ , where we assume that the control signal remains constant within each  $\Delta t'$ . Therefore, the resulting finite horizon optimization problem is defined as follows

$$\begin{aligned} & \underset{\bar{u}}{\text{minimize}} && H(\bar{u}) = H^1(\bar{u}) + H^2(\bar{u}) \\ & \text{subject to} && u_{o,s}^{c,\mu} \geq 0, \\ & && \sum_{s \in \mathcal{P}_o^c} u_{o,s}^{c,\mu} = \lambda. \end{aligned} \quad (22)$$

Note how there is no guarantee of convexity for  $H(\bar{u})$ . Therefore, we employed the *differential evolution heuristic global optimization algorithm* [30].

### B. Synthetic Network

We tested the model on the synthetic network shown in Fig. 1, where 1 and 8 are respectively the origin and destination nodes. For each arc  $L_\ell = 5[\text{km}]$ ,  $f_\ell(\rho \leq \hat{\rho}_\ell) = 80[\text{km/h}]$  and  $|f_\ell(\rho > \hat{\rho}_\ell)| = 30[\text{km/h}]$ . Each arc has a maximum density  $R_\ell = 100[\text{veh/km}]$ , except for arcs  $1 \rightarrow 2$  and  $7 \rightarrow 8$ , where  $R_{(1,2)} = R_{(7,8)} = 300[\text{veh/km}]$  to accentuate any possible congestion phenomena in the network. The network is discretized with  $\Delta x = 0.5[\text{km}]$ , leading to a grid of 10 cell on each edge and an associated  $\Delta t = 0.00625[\text{h}] (\simeq 23[\text{sec}])$  and one hour is simulated for a total of 160 time steps.

We define a single non-compliant class adopting an adaptive strategy as described in Section III with  $\theta^c = 0.5$  and  $\omega^c = 0.1$ . The associated inflow boundary condition at origin 1 corresponds to 4000[veh/h] up to time instant  $\nu = 100 (\simeq 37[\text{min}])$  and zero thereafter. The possible paths connecting the origin node with the destination are  $p_1 = [1, 2, 3, 5, 7, 8]$ ,  $p_2 = [1, 2, 4, 5, 7, 8]$  and  $p_3 = [1, 2, 4, 6, 7, 8]$ . We then define three compliant classes, each associated with one of the three paths. The control action is updated every 30 time steps ( $\simeq 11[\text{min}]$ ) until the input demand becomes zero. Then exploiting the equality constraint in (22) we obtain a total of 6 control variables.

Firstly, we compute the stochastic user equilibrium state considering only non-compliant users moving on the network. Fig 1 shows how, as expected, users are equally

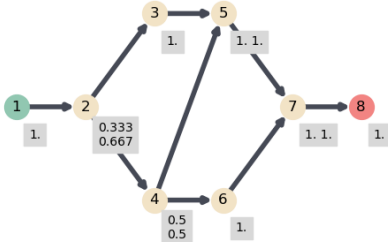


Fig. 1. Synthetic network. Next to each node are the distribution matrices at equilibrium.

distributed across all paths experiencing the same initial travel time of about  $0.31[h]$ .

Let us now consider a capacity loss on the last cell on arc  $4 \rightarrow 5$  after 30 time-steps ( $\simeq 11[\text{min}]$ ). As shown in fig. 2, after about 50 time steps ( $\simeq 19[\text{min}]$ ) almost all users avoid travelling along path  $p_2$  ( $TTT = 1675.8$ ). Three possible scenarios are then compared: *uncontrolled non adaptive*, *uncontrolled adaptive* and *controlled* ( $\lambda = 1$ ). Fig. 3 reports the average densities normalized over the maximum density for each arc in the three scenarios at time instant  $\nu = 100$  ( $\simeq 37[\text{min}]$ ), when the transitory phase ends while flow is still entering from node 1 and the congestion is at its peak. As expected, the worst-case scenario ( $TTT = 1675.8$ ) occurs when no control is applied and with users relying on a non-adaptive strategy. The average congestion on arc  $4 \rightarrow 5$  increases severely meanwhile the queue propagates backward onto links  $2 \rightarrow 4$  and  $1 \rightarrow 2$ . The overall network condition improves greatly when users apply an adaptive strategy ( $TTT = 1424.1$ ). Nevertheless, there is still significant congestion on arc  $4 \rightarrow 5$  and, more interestingly, on arch  $1 \rightarrow 2$ , because it is difficult to accommodate the demand accessing junction 2. Finally, in the third scenario where all vehicles are controlled ( $TTT = 1149.7$ ), following the disruption the average densities on all arcs remain sub-critical, with the exception of arc  $1 \rightarrow 2$  where, however, there is a decrease in the average saturation from 52% percent to around 40%, while the congestion on arc  $4 \rightarrow 5$  is completely dissipated.

Clearly, controlling all vehicles on the network delivers the best results. However, this eventuality is far from being

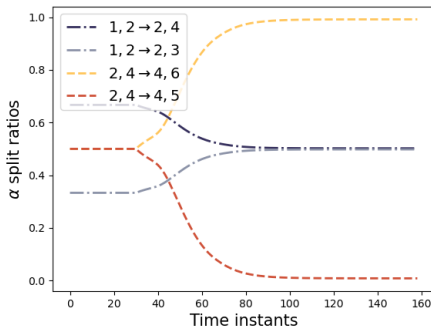


Fig. 2. Evolution over time of split ratios at nodes 2 and 4, uncontrolled adaptive scenario.

applicable in a real context. Therefore, it may be interesting to compare the results that can be obtained as the  $\lambda$  percentage of compliant users varies. Routing a fraction of users introduces the crucial challenge of having to account for the non-compliant users reaction within the control strategy, foreshadowing a Stackelberg game. We therefore consider three configurations: in *configuration 1*, users don't change their strategy, replicating the one adopted at the equilibrium meanwhile this information is known and exploited within the optimization process; in *configuration 2*, the optimization is still based on the user behaviour at the equilibrium, but non-compliant users adopt an adaptive strategy. Thus, there is a discrepancy between the behaviour actually adopted by the uncontrolled fraction of users and the information employed in the optimal routing computation; in *configuration 3* the non-compliant users adaptive strategy is known and actively employed in the optimization process.

Each configuration has been tested assuming any  $\lambda$  decimal value ranging from 0 to 1 for a total of 33 scenarios. In Fig. 4, the associated total travel time evolution is reported for each configuration. Naturally the result is the same ( $\pm 1$ ) when all vehicles are controlled ( $\lambda = 1$ ). At the opposite, when  $\lambda = 0$ , what matters is the behavior adopted by non-compliant users, since no control is performed. In all three configurations, increasing the percentage of controlled users improves the overall network performance, but with significant differences. In particular, it can be observed that systematically worse results are obtained in configuration 2 compared to configuration 3 (except, of course, for the two aforementioned extreme cases). In particular, the largest performance degradation is obtained in the interval  $\lambda \in [0.2, 0.5]$ . This is due to the fact that on the one hand the percentage of non-compliant users is still high while on the other hand a sub-optimal control based on inaccurate assumptions has the potential to perturb the system rerouting no less than 20% of the total flows. It is a delicate spot to be in, where the penalty to be paid as a result of inaccurate assumptions is significant and is likely to be extremely dependent on the network topology, making it difficult to estimate a priori. Such issue becomes less critical as the behavior of the non-

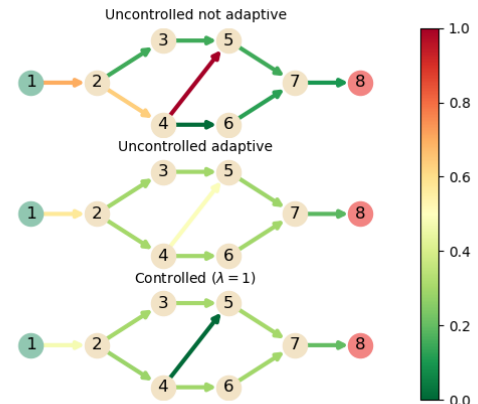


Fig. 3. Normalized average densities on arcs at time instant  $\nu = 80$ .

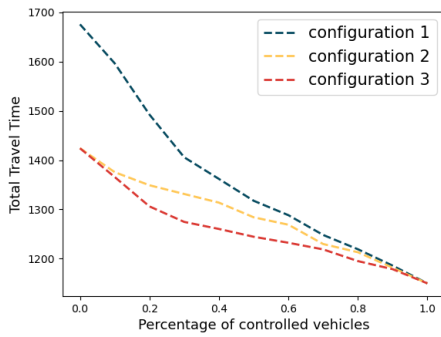


Fig. 4. Total travel time vs percentage of compliant users

compliant fraction of users gradually loses relevance as  $\lambda$  increases. Finally, regardless of the information available, the control action is still able to achieve better overall network performance than in the uncontrolled case.

## V. CONCLUSIONS

In this paper we have presented a dynamic macroscopic multi-population traffic model on road networks, able to represent different classes of users, each associated with a specific routing strategy. In particular, we distinguish between non-compliant and compliant classes, where the former represents users applying their individual wardropian equilibrium type strategy, while the latter consists of users inclined to follow a given pre-computed path. Therefore, we studied the impact of a control action while routing different fractions of users and with different level of information regarding the non-compliant users' autonomous behaviour. The results suggest how both the non-compliant users' behaviour and the assumption about it exploited within the optimization affect significantly the effectiveness of the control action. Future work aims to implement the model on a more realistic network and to investigate the effectiveness of a control strategy in relation to the user behaviour and the topological functional characteristics of the network itself.

## REFERENCES

- [1] D. K. Merchant and G. L. Nemhauser, "A model and an algorithm for the dynamic traffic assignment problems," *Transportation science*, vol. 12, no. 3, pp. 183–199, 1978.
- [2] D. K. Merchant and G. L. Nemhauser, "Optimality conditions for a dynamic traffic assignment model," *Transportation Science*, vol. 12, no. 3, pp. 200–207, 1978.
- [3] J. G. Wardrop, "Some theoretical aspects of road traffic research.," *Proceedings of the Institution of Civil Engineers*, vol. 1, no. 3, pp. 325–362, 1952.
- [4] A. Festa, P. Goatin, and F. Vicini, "Navigation system based routing strategies in traffic flows on networks." working paper or preprint, Mar. 2023.
- [5] M. Carey and D. Watling, "Dynamic traffic assignment approximating the kinematic wave model: System optimum, marginal costs, externalities and tolls," *Transportation Research Part B: Methodological*, vol. 46, no. 5, pp. 634–648, 2012.
- [6] S. Samaranayake, J. Reilly, W. Krichene, M. L. Delle Monache, P. Goatin, and A. Bayen, "Discrete-time system optimal dynamic traffic assignment (SO-DTA) with partial control for horizontal queuing networks," *Transportation Science*, 2018.
- [7] Y. A. Korilis, A. A. Lazar, and A. Orda, "Achieving network optima using stackelberg routing strategies," *IEEE/ACM transactions on networking*, vol. 5, no. 1, pp. 161–173, 1997.

- [8] C. Swamy, "The effectiveness of stackelberg strategies and tolls for network congestion games," *ACM Transactions on Algorithms (TALG)*, vol. 8, no. 4, pp. 1–19, 2012.
- [9] S. Samaranayake, J. Reilly, W. Krichene, J. B. Lespiau, M. L. D. Monache, P. Goatin, and A. Bayen, "Discrete-time system optimal dynamic traffic assignment (SO-DTA) with partial control for horizontal queuing networks," in *2015 American Control Conference (ACC)*, pp. 663–670, July 2015.
- [10] S. Chanut and C. Buisson, "Macroscopic model and its numerical solution for two-flow mixed traffic with different speeds and lengths," *Transportation Research Record: Journal of the Transportation Research Board*, no. 1852, pp. 209–219, 2003.
- [11] S. Fan and D. B. Work, "A heterogeneous multiclass traffic flow model with creeping," *SIAM Journal on Applied Mathematics*, vol. 75, no. 2, pp. 813–835, 2015.
- [12] S. Gashaw, P. Goatin, and J. Härrri, "Modeling and analysis of mixed flow of cars and powered two wheelers," *Transportation Research Part C: Emerging Technologies*, vol. 89, pp. 148–167, 2018.
- [13] M. W. Levin and S. D. Boyles, "A multiclass cell transmission model for shared human and autonomous vehicle roads," *Transportation Research Part C: Emerging Technologies*, vol. 62, pp. 103 – 116, 2016.
- [14] J. Van Lint, S. Hoogendoorn, and M. Schreuder, "Fastlane: New multiclass first-order traffic flow model," *Transportation Research Record: Journal of the Transportation Research Board*, no. 2088, pp. 177–187, 2008.
- [15] M. Garavello and B. Piccoli, "Source-destination flow on a road network," *Commun. Math. Sci.*, vol. 3, no. 3, pp. 261–283, 2005.
- [16] E. Cristiani and F. S. Priuli, "A destination-preserving model for simulating Wardrop equilibria in traffic flow on networks," *Netw. Heterog. Media*, vol. 10, no. 4, pp. 857–876, 2015.
- [17] A. Festa and P. Goatin, "Modeling the impact of on-line navigation devices in traffic flows," in *2019 IEEE 58th Conference on Decision and Control (CDC)*, pp. 323–328, 2019.
- [18] M. J. Lighthill and G. B. Whitham, "On kinematic waves II. a theory of traffic flow on long crowded roads," *Proc. R. Soc. Lond. A*, vol. 229, no. 1178, pp. 317–345, 1955.
- [19] C. F. Daganzo, "The cell transmission model: A dynamic representation of highway traffic consistent with the hydrodynamic theory," *Transportation Res. Part B*, vol. 28, no. 4, pp. 269–287, 1994.
- [20] S. K. Godunov, "A difference method for numerical calculation of discontinuous solutions of the equations of hydrodynamics," *Mat. Sb. (N.S.)*, vol. 47 (89), pp. 271–306, 1959.
- [21] J. Lebacque, "The Godunov scheme and what it means for first order traffic flow models," in *Proceedings of the 13th International Symposium on Transportation and Traffic Theory, Lyon, France, July*, vol. 2426, 1996.
- [22] R. Courant, K. Friedrichs, and H. Lewy, "Über die partiellen Differenzgleichungen der mathematischen Physik," *Math. Ann.*, vol. 100, no. 1, pp. 32–74, 1928.
- [23] M. Garavello, K. Han, and B. Piccoli, *Models for vehicular traffic on networks*, vol. 9. American Institute of Mathematical Sciences (AIMS), Springfield, MO, 2016.
- [24] M. L. Delle Monache, P. Goatin, and B. Piccoli, "Priority-based Riemann solver for traffic flow on networks," *Commun. Math. Sci.*, vol. 16, no. 1, pp. 185–211, 2018.
- [25] C. F. Daganzo and Y. Sheffi, "On stochastic models of traffic assignment," *Transportation science*, vol. 11, no. 3, pp. 253–274, 1977.
- [26] A. Hagberg, P. Swart, and D. S. Chult, "Exploring network structure, dynamics, and function using networkx," tech. rep., Los Alamos National Lab.(LANL), Los Alamos, NM (United States), 2008.
- [27] C. R. Harris, K. J. Millman, S. J. van der Walt, R. Gommers, P. Virtanen, D. Cournapeau, E. Wieser, J. Taylor, S. Berg, N. J. Smith, R. Kern, M. Picus, S. Hoyer, M. H. van Kerkwijk, M. Brett, A. Haldane, J. F. del Río, M. Wiebe, P. Peterson, P. Gérard-Marchant, K. Sheppard, T. Reddy, W. Weckesser, H. Abbasi, C. Gohlke, and T. E. Oliphant, "Array programming with NumPy," *Nature*, vol. 585, pp. 357–362, Sept. 2020.
- [28] T. pandas development team, "pandas-dev/pandas: Pandas," Feb. 2020.
- [29] T. S. development team, "SciPy 1.0: Fundamental Algorithms for Scientific Computing in Python," *Nature Methods*, vol. 17, pp. 261–272, 2020.
- [30] R. Storn and K. Price, "Differential evolution—a simple and efficient heuristic for global optimization over continuous spaces," *Journal of global optimization*, vol. 11, no. 4, p. 341, 1997.